1400059

7

CAMBRIDGE UNIVERSITY PRESS

North American Branch
32 Avenue of the Americas
New York, NY 10013-2473, USA

Tel : 212 337-5978
Fax : 212 337-5959
E-mail: mgillette@cambridge.org

PROOFREADING INSTRUCTIONS

Dear *Microscopy and Microanalysis* Contributor:

Attached is a PDF page proof of your introduction/article/book review scheduled to be published in:

Microscopy and Microanalysis

Please follow these procedures:

1. **Proofreading**: Proofread your article carefully. Check especially the spellings of names and places as well as the accuracy of dates and numbers. Please answer all queries that may appear on a separate page.

2. **Text**: Changes in the text are limited to typographical and factual errors. Rewriting or other stylistic changes are not permitted. Contributors may be charged for excessive author alterations, and publication of your article may be delayed.

3. **Corrections**: Please respond with an e-mail message to Morrell Gillette at mgillette@cambridge.org, identifying the correction by page number, column, paragraph, and line. Please indicate the present errant copy followed by the correct copy. The corrections to the proofs should be sent within 2 days of receipt. Corrections can also be entered into the PDF as embedded comments.

4. **References**: If the query involves a reference entry, please arrange the new entry into the correct format. In order to prepare the HTML full-text files for online viewing, the complete information including correct spelling of author names, year, titles, publisher, city of publication, page range, and so forth are needed.

5. **Figures**: Review the figure reproductions on the page proofs to see if important features have been well represented. If something seems out of order, indicate the errant features in a cover letter. Should it be necessary that new electronic copy of the figures (in PDF, TIFF, or EPS) or text (Word or LaTeX) will have to be provided, please indicate which application is being used.

6. **Offprints or Bound Copies**: Free offprints are longer being offered. However, a message with a link to access a free PDF of your paper will be sent to you. To order reprints or offprints of your article or printed copies of the issue, please visit the Cambridge University Reprint Order Center online at: www.sheridan.com/cup/eoc

7. **Delay in response**: Please note that failure to respond in a timely fashion may delay publication of your article or may require publication without your corrections. Thank you for your prompt attention to these proofs. If you have any questions, please feel free to contact Morrell Gillette by e-mail: mgillette@cambridge.org, or at (212) 337-5978. Thanks.

Best Regards,
Morrell Gillette,
Production Editor

QUERY FORM

MAM	
Manuscript ID	**[Art. Id: 1400059]**
Author	
Editor	
Publisher	

Journal: Microscopy And Microanalysis

Author :- The following queries have arisen during the editing of your manuscript. Please answer queries by making the requisite corrections at the appropriate positions in the text.

Query No	*Nature of Query*
Q1	The distinction between surnames can be ambiguous, therefore to ensure accurate tagging for indexing purposes online (eg for PubMed entries), please check that the highlighted surnames have been correctly identified, that all names are in the correct order and spelt correctly.
Q2	Please provide manufacturer details for Hitachi, Gatan Enfina, Nion UltraSTEM.
Q3	Please provide volume number and page range in Ref. Carretero-Genevrier et al. (2013).
Q4	Please provide last page number in Ref. Luo et al. (2009), if applicable.

Cambridge University Press

Microsc. Microanal. 00, 1–7, 2014
doi:10.1017/S1431927614000592

Microscopy AND Microanalysis

Electronic and Magnetic Structure of LaSr-2 × 4 Manganese Oxide Molecular Sieve Nanowires

Jaume Gazquez,[1,*] Adrián Carretero-Genevrier,[2,3] Martí Gich,[1] Narcís Mestres,[1] and María Varela[4,5]

[1]*Institut de Ciència de Materials de Barcelona ICMAB, Consejo Superior de Investigaciones Científicas CSIC, 08193 Bellaterra, Spain*
[2]*Laboratoire Chimie de la Matière Condensée, UMR UPMC-Collège de France-CNRS 7574, Collège de France, 11 Place Marcelin Berthelot, 75231 Paris, France*
[3]*Institut des Nanotechnologies de Lyon (INL) CNRS - Ecole Centrale de Lyon., 36 avenue Guy de Collongue, 69134 Ecully*
[4]*Materials Science and Technology Division, Oak Ridge National Laboratory, Oak Ridge, Tennessee 37831, USA*
[5]*Departamento de Física Aplicada III & Instituto Pluridisciplinar, Universidad Complutense de Madrid, Madrid 28040, Spain*

Abstract: In this study we combine scanning transmission electron microscopy, electron energy loss spectroscopy and electron magnetic circular dichroism to get new insights into the electronic and magnetic structure of LaSr-2 × 4 manganese oxide molecular sieve nanowires integrated on a silicon substrate. These nanowires exhibit ferromagnetism with strongly enhanced Curie temperature ($T_c > 500$ K), and we show that the new crystallographic structure of these LaSr-2 × 4 nanowires involves spin orbital coupling and a mixed-valence Mn^{3+}/Mn^{4+}, which is a must for ferromagnetic ordering to appear, in line with the standard double exchange explanation.

Key words: EELS, STEM, nanoparticles, nanowires, manganese molecular sieves, white lines, oxidation state

Introduction

Magnetic oxide nanoparticles are interesting for a wide range of novel devices since they constitute the building blocks for future data storage devices or magnetic sensors. However, for practical device applications, magnetic nanomaterials should exhibit a T_c well above room temperature. Many complex oxides, such as mixed-valence perovskite manganites, diluted magnetic oxides, spinels or ferrites, exhibit this requirement in bulk. However, increasing T_c values above room temperature in nano-systems remains a challenge, since the physical properties of nanostructures often differ from those exhibited by their bulk counterparts. We have recently been able to synthesize manganese oxide molecular sieve nanowires that display ferromagnetism above room temperature using a sol–gel-based polymeric precursor solution and track-etched polymer templates (Carretero-Genevrier et al., 2011, 2008). Unfortunately, a microscopic explanation of the underlying physics is lacking. This is, in part, due to the fact that the magnetic characterization properties are based on macroscopic measurements of a large number of nanostructures, and one cannot relate the local structure of a single nanowire with its actual averaged magnetic properties, so the nature of magnetism in the nanometer scale is still unknown.

In order to gain further knowledge in this front, real space probes with atomic resolution and sensitivity to magnetic quantities are needed. Among the experimental techniques available for characterization of nanostructured materials, aberration corrected scanning transmission electron microscopy (STEM), in combination with electron energy loss spectroscopy (EELS), is a powerful technique for structural and chemical analysis down to the atomic scale. The STEM electron probe routinely yields spatial resolution of < 1 Å as well as increased contrast both in imaging and in spectroscopy (Varela et al., 2004, 2005), allowing simultaneous mapping of the structure, chemistry, and electronic properties of materials in a single experiment. Furthermore, as has recently been demonstrated by Schattschneider et al. (2006) electron probes can also be used to study the magnetic properties. Energy-loss magnetic circular dichroism (EMCD) can be measured in a TEM studying the $L_{2,3}$ EELS absorption edges of transition metal, and has already been used to study nanostructured materials in the sub-nanometer range (Schattschneider et al., 2008; Zhang et al., 2009, 2011; Lidbaum et al., 2010; Carretero-Genevrier et al., 2012; Salafranca et al., 2012).

In this work, we will shed some light on the connection between structure, chemistry, and magnetism in the nanometer scale in manganese oxide molecular sieve nanowires. Our LaSr-2 × 4 nanowires present a T_c that is much higher than most perovskite Mn oxides (above 500 K) so they can be studied at room temperature in the aberration corrected STEM. We will use atomic resolution STEM-EELS to investigate the electronic properties of different Mn sites within the monoclinic structure and combine them with EMCD onto a single LaSr-2 × 4 nanowire and attempt to distinguishing the Mn spin and orbit contribution. Our results will pave the way to elucidate the mechanism underlying both ferromagnetism and the high Curie temperature exhibited by these LaSr-2 × 4 nanowires.

Received September 28, 2013; accepted February 23, 2014
*Corresponding author. jgazqueza@gmail.com

Materials and Methods

LaSr-2 × 4 nanowires were prepared from 1 M aqueous solutions composed of $La(NO_3)3•6\ H_2O$, $Sr(NO3)2•4\ H_2O$ and $Mn(NO_3)2•4\ H_2O$ in the molar proportion of 07:0.3:1, respectively. The addition of ethylene glycol (EG) heated above 100°C promotes polymerization of the EG in order to reach the optimum viscosity value required for filling of the template's pores.

Track etched polymer templates were prepared by irradiation of polyimide or polycarbonate directly supported on single crystalline Si substrates by using heavy ions and posterior chemical development as described elsewhere (Carretero-Genevrier et al., 2010, 2011, 2012, 2013). Then, all precursor solutions were used to fill the nanopores of the polymer template. A thermal treatment at 800°C for 5 h (temperature ramp 3°C min-1) in air was applied directly after filling the nonporous template in a tubular furnace in order to obtain vertical epitaxial LaSr-2 × 4 nanowires on a silicon substrate. ε-MnO_2 nanowires up to 30 μm in length, were synthesized following the same procedure with a thermal treatment of 2 h at 700°C. These nanowires were indexed with a hexagonal unit cell $a = b = 5.28$ Å, $c = 2.86$ Å, $\alpha = 90°$, $\beta = 90°$ and $\gamma = 120°$, described elsewhere (Carretero-Genevrier et al., 2011).

The samples' microstructure was investigated using a field emission gun scanning electron microscope (FEG-SEM), Hitachi's SU77. A VG Microscope HB501UX and a Nion UltraSTEM, both operated at 100 kV and equipped with a Nion aberration corrector and a Gatan Enfina EEL spectrometer, were used for high-resolution imaging, Z-contrast imaging, and STEM-EELS spectrum imaging. The probe forming aperture had a semiangle of ~ 25 mrad. The collection angle at the spectrometer was estimated to be 12 mrad. Thin foil *cross-sectional* samples of the wires grown on the substrates were prepared for STEM by conventional grinding and ion milling methods. The EMCD experiment was also carried out using a Nion Ultrastem at 100 kV, but operated in nanodiffraction mode. In this mode the scanning beam has a diameter of about 1 nm. The convergence and collection semiangles were set to 30 and 34 mrad, respectively. The detection of circular dichroism in the TEM is described in the literature (Schattschneider et al., 2006). It can be achieved by recording two EEL spectra in the diffraction plane with different *polarizations*, this is, having an opposite sign of the imaginary part, I + and I −, by selecting the scattering angles such that the momentum transfers q and q′ are orthogonal to each other, q⊥q′.

Results and Discussion

Our nanowires are magnetic at room temperature. The proposed unit cell of these nanowires is monoclinic with lattice parameters $a = 13.8$ Å, $b = 5.7$ Å, $c = 21.8$ Å, and $\beta = 101°$, where the long axis of the nanowires is along the b crystallograghic direction (Carretero-Genevrier et al., 2008). It also presents an ordered arrangement of the La^{3+} and Sr^{2+} cations (Carretero-Genevrier et al., 2011). Figure 1a–1c show a low magnification FEG-SEM image of the LaSr-2 × 4

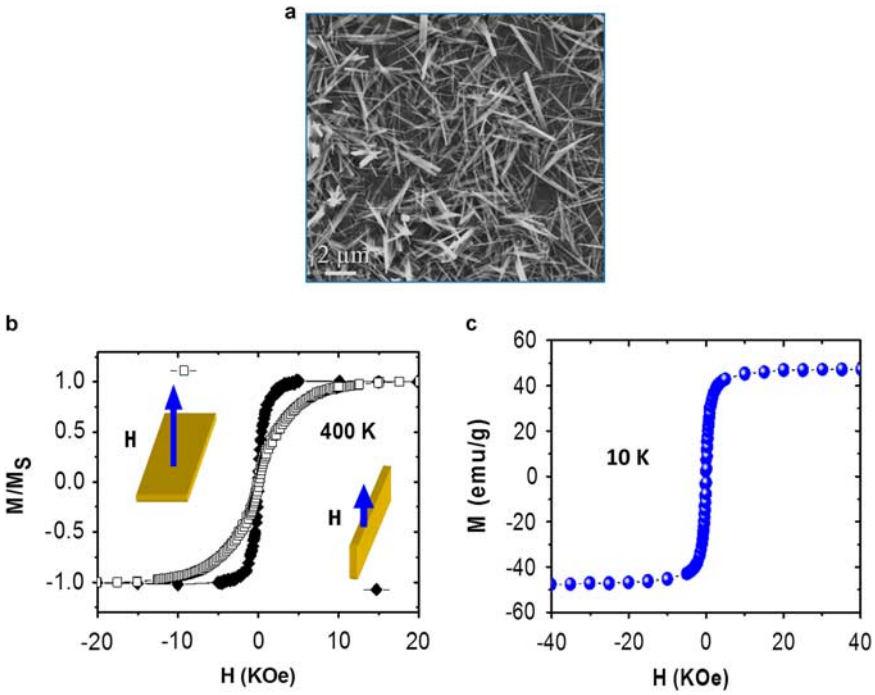

Figure 1. a: Low magnification field emission gun scanning electron microscope (FEG-SEM) image of LaSr-2 × 4 nanowires epitaxially grown on a α-quartz/Si substrate. **b**: Hysteresis loops of the LaSr-2 × 4 nanowires measured at 400 K for fields applied parallel (filled symbols), and perpendicular (open symbols), to the substrate plane. **c:** Hysteresis loops of the LaSr-2 × 4 nanowires measured at 10 K, showing a saturation magnetization of (Ms) of 47 ± 10 emu/g.

nanowires and the magnetic hysteresis loops measured for fields up to 5 T, at 400 K and at 10 K, respectively. For the 400 K measurement, the magnetic field was applied in-plane and out-of-plane with respect to the substrate. The out-of plane magnetization curve saturates at a higher magnetic field than does the in-plane curve, indicating that the direction perpendicular to the long axis of the nanowires is a hard magnetic axis. We have calculated the saturation magnetization value for the monoclinic LaSr-2×4 nanowires. The mass of nanowires was estimated in $2.86 \cdot 10^{-06}$ g, which gives a saturation magnetization of 47 ± 10 emu/g for the LaSr-2×4 monoclinic phase at 10 K, which is half of the saturation magnetization value of the $La_{0.7}Sr_{0.3}MnO_3$ bulk perovskite (90 emu/g), indicating the high ferromagnetic strength of this novel type of nanostructure. Considering the structure proposed by Carretero-Genevrier et al. (2011), which is similar to the RUB-7 manganese oxide structure (Rziha et al., 1996), one can estimate for the LaSr-2×4 nanowires a 1.8 μ_B/Mn, slightly less than half of that of Mn^{3+}, 4.9 μ_B.

Figure 2a shows a typical cross-sectional low magnification high-angle annular dark field image STEM image of one of our samples. The brighter rods correspond to the randomly oriented LaSr-2×4 nanowires, which cover the surface of a polycrystalline α-quartz layer formed along with the nanowire synthesis. Figure 2b is a high resolution TEM image showing a LaSr-2×4 nanowire epitaxially grown on top of an α-quartz grain. The Fast Fourier transform (FFT) of Figure 2b reveals that the orientation relationship can be described as (010) LaSr-2×4//(010) α-quartz and an in-plane epitaxial relationship given by [20-2] LaSr-2×4// [-101] α-quartz. STEM-EELS studies allowed us to explore the chemistry of the nanowires. Figure 2c shows an EEL spectrum generated from scanning a nanowire, confirming its uniform composition. It is worth noting that neither appreciable inter-diffusion of Si into the nanowires nor any trace of Sr on the quartz layer was detected from our EELS studies.

The crystal quality of the wires is high. The growth process of these LaSr-2×4 nanowires on Si substrates has been well established in recent works (Carretero-Genevrier et al., 2008, 2011, 2013). The confinement imposed by a polymer template during thermal treatment results in the formation of ε-MnO_2 nanoparticles in the early stages of the growth process. These act as seeds for the further growth of

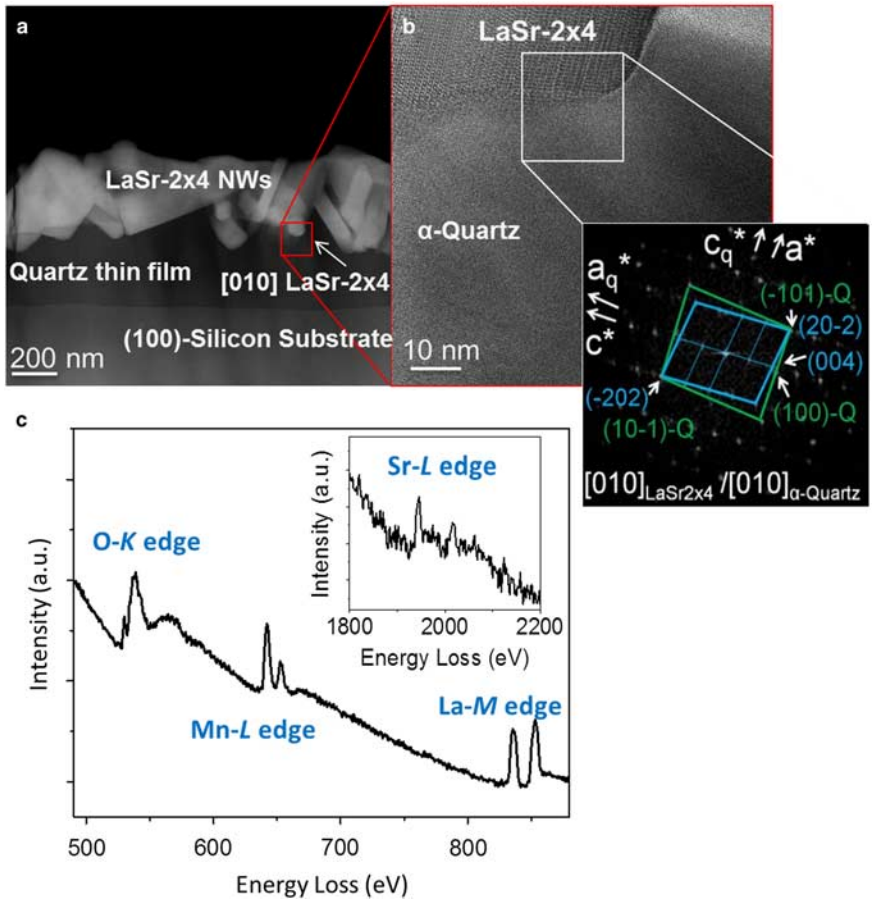

Figure 2. a: Low magnification Z-contrast image of LaSr-2×4 nanowires epitaxially grown on an α-quartz/Si substrate. The inset shows the FFT of both phases. **b**: High-resolution transmission electron microscopy (HRTEM) image of the α-quartz-Si interface along [010] α-quartz zone axis. **c**: Electron energy loss (EEL) spectrum generated from the EELS scans across a nanowire.

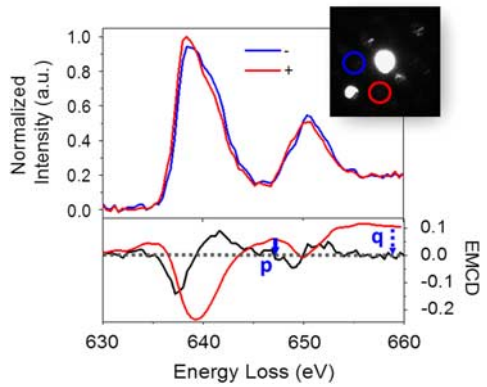

Figure 3. Mn $L_{2,3}$ edges, after background subtraction, in the two configurations (+) and (−), and the resultant dichroic signal (upper and bottom panels, respectively). The spectra were normalized to the background region between the two edges. The inset shows the diffraction pattern and the detector positions used. The electron energy loss spectroscopy (EELS) spectrum has been corrected by the subtraction of a baseline (a double-step function) that takes into account a linear increase of the background inside the $L_{2,3}$ edges, as well as the background out of the $L_{2,3}$ edge. The red line is the integral for the signal. Blue arrows indicate the values of p and q.

the manganate nanowires at high temperature treatments (i.e. 800°C). In addition, contact of the silica native layer with alkaline-earth metal cations (like the Sr^{2+} present in the precursor solution) during the thermal treatment yields its devitrification to an α-quartz layer, as recently demonstrated by the authors (Carretero-Genevrier et al., 2013). This is a key factor for stabilization of these manganese oxide nanowires. Indeed, α-quartz film renders better lattice matching to the complex oxide nanostructures favoring the epitaxial growth of the LaSr-2 × 4 nanowires. However, due to the relatively low annealing temperature (800°C), the α-quartz layer grown on Si substrates is polycrystalline, which results in growth of the nanowires along different orientations with respect to the substrate plane.

The magnetism of these nanowires can be studied using EMCD, which, as mentioned before, can be measured in a TEM studying $L_{2,3}$ EELS absorption edges of transition metals (Schattschneider et al., 2006). Following the procedures described by Schattschneider et al., we have obtained the Mn-L edges from two conjugated spots in the nanodiffraction diagram, which are equivalent to the two beam polarizations used in X-ray magnetic circular dichroism (XMCD) measurements (Fig. 3a). The dichroic signal is then given by the difference between these two spectra. A clear dichroism is observed in the LaSr-2 × 4 nanowire, as displayed in the lower panel of Figure 3a. Further evidence of the difference in Mn $L_{2,3}$ edges comes from calculating the $L_{2,3}$ ratio for each spectrum coming from the two conjugated spots in the diffraction pattern. The value of the $L_{2,3}$ ratio has been obtained here using the second derivative method (Botton et al., 1995), giving the values 2.4 and 2.9 for positions (+) and (−), respectively. EEL spectra were acquired from relatively thin regions, with a thickness value in terms of the inelastic mean-free path of $t/\lambda < 0.5$.

Quantification of the actual values of the spin and orbital moments for the Mn ions is challenging. However, the EMCD integrals might supply information about their relative size and orientation. We have used two different methods to calculate the quotient between the orbital (l_Z) and spin (s_Z) moments projections: the approach followed by Chen et al. for X-rays and that used by Calmels et al. (Chen et al., 1995; Calmels et al., 2007), which takes into account the dynamical diffraction effects arising from the propagation of the electron diffracted beams within the crystal (something that cannot be omitted in a quantitative analysis). First, we consider the use of the sum rules (Chen et al., 1995), which may provide the relative size and orientation of the s_Z and l_Z moments of Mn. Figure 3b displays the result of applying sum rules to Mn ions on the LaSr-2 ×4 nanowires. Bear in mind that the only XMCD expression that can be applied in our experiment is for the ratio of the orbital and the spin moment. q and p are the values of the integrated areas of the EMCD signal of the Mn $L_{2,3}$ edges and the L_3 edge, respectively (Fig. 3b). The obtained value for the quotient l_Z/s_Z is −0.82. The negative value points to an antiparallel alignment of the spin and the orbital magnetic moments.

These results can be compared with those obtained using the sum rules derived for EMCD spectra, which take into account dynamical effect, sample orientation, and thickness (Calmels et al., 2007). Following the procedure described by Calmels et al., (2007) and having integrated the EMCD spectrum in the energy windows [632 eV, 644 eV] for the L_3 edge and [646 eV, 657 eV] for the L_2 edge, the measurement then gives $l_Z/s_Z = -0.62$. This result is in agreement with the value previously obtained.

In order to get new insights into the mechanism responsible for the high temperature ferromagnetism we studied and compared the electronic structure of these LaSr-2 × 4 nanowires with that of the ε-MnO_2 phase, which is nonmagnetic, has a unique Mn valence value and, as mentioned before, serves as a seed for the growth of the manganite nanowires. In manganites, the small peak in the very onset of the O-K edge is related to the hybridization of the O 2p band and the Mn 3d states, and it is found to change with manganese oxidation state (Varela et al., 2009). In addition, as confirmed by several studies, the ratio between L_3 and the L_2 of the $L_{2,3}$ edge also changes as a function of the occupancy of the Mn 3d orbitals, and can be used as a fingerprint for transition metal valence (Rask et al., 1987; Botton et al., 1995; Nakagawa et al., 2006; Varela et al., 2009). Accordingly, these two different features, the O-K edge pre-peak intensity and the Mn $L_{2,3}$ ratio have been used to characterize the Mn oxidation state of our samples.

Figures 4a and 4b show a comparison of O-K and Mn-L EEL spectra for ε-MnO_2 (in black) and LaSr-2 × 4 nanowires (in red), which show evident differences between these two phases. For the LaSr-2 × 4 nanowires, the O-K edge pre-peak (peak A) is significantly suppressed and shifted to higher

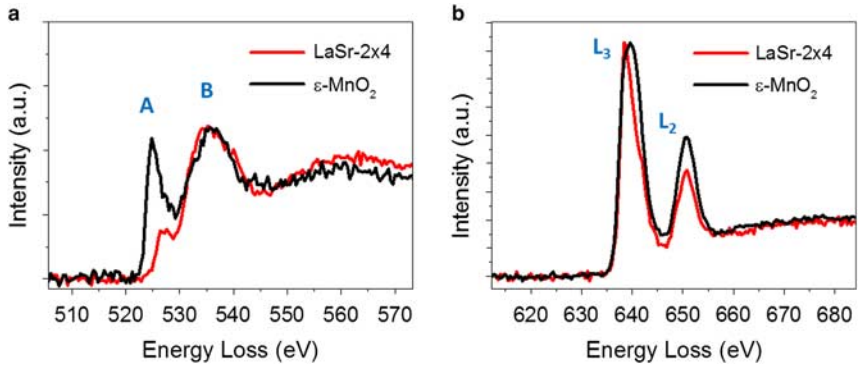

Figure 4. **a** and **b**: O-*K* edge and Mn-*L* edge averaged electron energy loss (EEL) spectra of a ε-MnO_2 nanowire (in black) and a LaSr-2 × 4 nanowire (in red), respectively.

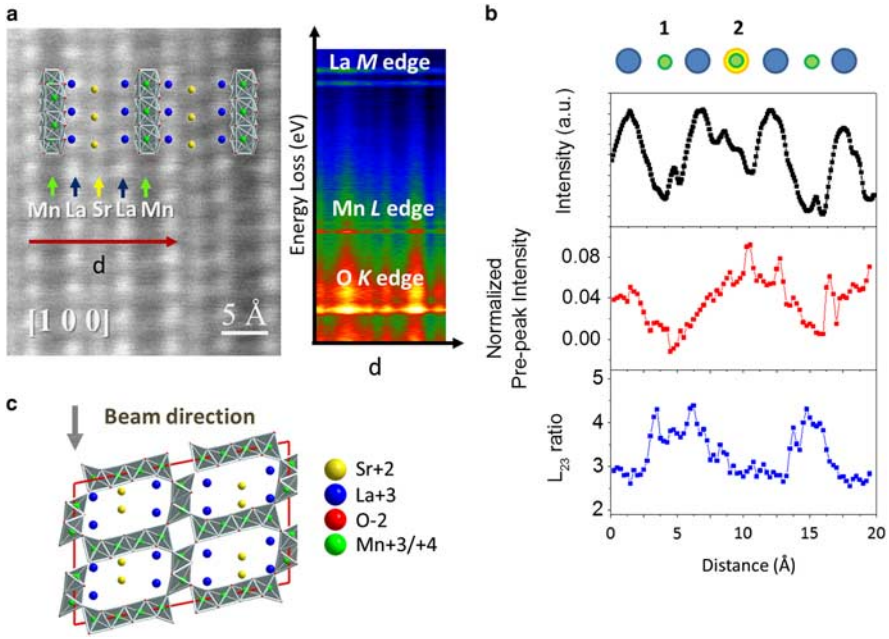

Figure 5. **a**: Left panel: High resolution Z-contrast image of a LaSr-2 × 4 nanowire along the [100] zone axis. A LaSr-2 × 4 nanowire cell model has been highlighted on the Z-contrast image, with yellow circles marking the Sr columns position, blue circles the La column position, and red and green circles the O and Mn positions, respectively. Right panel: EELS data acquired in a line scan showing the evolution along different planes of the LaSr-2 × 4 nanowire of the O-*K*, Mn-*L* and La-*M* edges along the red arrow on **a**. Red arrow indicates the direction of the scan. **b**: From top to bottom, annular dark field (ADF) simultaneous signal intensity, normalized pre-peak intensity of the O-*K* edge and $L_{2,3}$ ratio profiles along the direction of the red arrow in panel **a**. Positions 1 and 2 mark two different Mn sites. **c**: A drawing of the model of the LaSr-2 × 4 nanowire unit cell along [010] (Carretero-Genevrier et al., 2011), with the relative direction of the electron beam during the scanning.

energies compared with the center peak (peak B). Both the intensity and the distance (ΔE) between peak A and B are an accurate indicator of valence change (Luo et al., 2009; Varela et al., 2009). Also, analysis of the Mn $L_{2,3}$ edge confirms the change of manganese oxidation state. The resulting $L_{2,3}$ ratios have values of 2 and 3.2 for ε-MnO_2 and LaSr-2 × 4 nanowires, respectively. According to previous reports, the $L_{2,3}$ ratio increases with the oxidation of manganite perovskites (Varela et al., 2009). Hence, doping the ε-MnO_2 nanowires with La and Sr cations induces a mixed-valence Mn^{3+}/Mn^{4+} as in perovskite manganites, This mixed valence state may be associated with double exchange and result in long range ferromagnetism (Dagotto et al., 2001). Also, the particular atomic arrangement of the Mn^{3+}/Mn^{4+} manganese atoms within the monoclinic structure may change the interatomic distances and modify the exchange interaction stabilizing a ferromagnetic configuration.

Further evidence of the mixed-valence state of the LaSr-2 × 4 comes from spectrum imaging. Figure 5 displays a set of data used to extract the local variation of the Mn

oxidation state. Figure 5a shows a high-resolution Z-contrast image of the LaSr-2 × 4 nanowire along its [100] zone axis, together with a line scan along the [001] axis. The ripples in the O, La, and Mn signals along the scan line are a reflection of the positions of the elements. A model structure, overlaid on the Z-contrast image, was proposed in a previous work from a similar line scan (Carretero-Genevrier et al., 2011). Figure 5c shows the proposed structure of the LaSr-2 × 4 nanowires viewed along its *b*-axis and its relative orientation with respect to the electron beam during the EEL scan. In this work, we have used a line scan with a longer acquisition time, 1 s per pixel, to probe the changes in the fine structure at different atomic positions. We have used the normalized O-*K* pre-peak intensity (compared with the center O-*K* edge peak, B) and the Mn $L_{2,3}$ ratio to characterize our sample (Fig. 4). The spatial modulation observed on both signals is the fingerprint for a local variation of the Mn oxidation state. When the scanning probe steps on the Mn column that has La cations as first neighbors (position 1 in Fig. 5b) the normalized pre-peak intensity decreases while the $L_{2,3}$ ratio increases. On the other hand, when the probe steps on the Sr/Mn column (position 2 in Figure Fig. 5b) the normalized pre-peak intensity increases and the $L_{2,3}$ ratio decreases. Comparing these results with those obtained from the ε-MnO_2 phase (Fig. 4) one can state that the Mn cations surrounded by La (position 1) have a lower oxidation compared with those found in position 2.

Summary and Conclusions

In summary, using EMCD we have studied the magnetism of a single LaSr-2 × 4 nanowire at room temperature. The nanowires are ferromagnetic and EMCD measurements show that there is a significant orbital component to the magnetic moment and that it is aligned antiparallel to the spin moment. These results suggest a strong spin orbit coupling, since oppositely oriented dipole moments have lower energy than those aligned parallel with each other. Our finding suggests, as expected from the third Hund rule, that Mn shells are less than half-filled, and that the origin of ferromagnetism may reside in a double-exchange-like mechanism. Indeed, spatially resolved EELS confirms the presence of mixed-valence Mn cations at different sites as a result of the ordered arrangement of the La^{3+} and Sr^{2+} cations within the structure. However, the electronic structure of these monoclinic LaSr-2 × 4 nanowires differs from its perovskite-like counterparts and the fine structure of the O-*K* edge presents significant changes compared with manganites (Luo et al., 2009; Varela et al., 2009). Although the pre-peak in the O-*K* edge of manganites measures the electronic occupancy of the hybridized O 2*p* and Mn 3*d* states, and hence the oxidation state of the Mn, the lattice effects must play a key role in the structure of the O-*K* edge in the case of the LaSr-2 × 4 nanowires. The different disposition and arrangement of La and Sr cations in the new structure of the nanowires may well affect the Mn-O bonds of MnO_6 octahedra. While further work is needed on the theoretical side to interpret the features of the electronic structure of our nanowires, our results pave the way toward harnessing the strong magnetism at room temperature measured in LaSr-2 × 4 manganese oxide molecular sieve nanowires.

Acknowledgments

We acknowledge the financial support from MICINN (MAT2008-01022, Consolider NANOSELECT CSD 2007-00042). We thank Etienne Ferain and it4ip company for supplying the nanoporous polymer membranes. Work at ORNL was supported by the Office of Science, Materials Sciences and Engineering Division of the U.S. Department of Energy (M.V.). A.C.G. acknowledges the financial support from Collège de France foundation, LCMCP for his Visiting Scientist position and INL-CNRS for his detachment. We thank David Montero and IMPC for use of the FEG-SEM facilities. J.G. is thankful for financial support from the European Research Council Starting Investigator Award, grant no. 239739 STEMOX and from the Spanish Government (RyC-2012-11709). M.G. Acknowledges the Spanish Government (RyC-2009-04335 contract).

References

Botton, G.A., Appel, C.C., Horsewell, A. & Stobbs, W.M. (1995). Quantification of the EELS near-edge structures to study Mn doping in oxides. *J Microsc* **180**, 211–216.

Calmels, L., Houdellier, F., Warot-Fonrose, B., Gatel, C., Hÿtch, M., Serin, V., Snoeck, E. & Schattschneider, P. (2007). Experimental application of sum rules for electron energy loss magnetic chiral dichroism. *Phys Rev B* **76**, 060409.

Carretero-Genevrier, A., Gázquez, J., Idrobo, J.C., Oró, J., Arbiol, J., Varela, M., Ferain, E., Rodríguez-Carvajal, J., Puig, T., Mestres, N. & Obradors, X. (2011). Single crystalline $La_{0.7}Sr_{0.3}MnO_3$ molecular sieve nanowires with high temperature ferromagnetism. *J Am Chem Soc* **133**, 4053–4061.

Carretero-Genevrier, A., Gazquez, J., Magén, C., Varela, M., Ferain, E., Puig, T., Mestres, N. & Obradors, X. (2012). Chemical synthesis of oriented ferromagnetic LaSr-2 × 4 manganese oxide molecular sieve nanowires. *Chem Commun (Camb)* **48**, 6223–6225.

Carretero-Genevrier, A., Gázquez, J., Puig, T., Mestres, N., Sandiumenge, F., Obradors, X. & Ferain, E. (2010). Vertical $(La,Sr)MnO_3$ nanorods from track-etched polymers directly buffering substrates. *Adv Functional Mater* **20**, 892–897.

Carretero-Genevrier, A., Gich, M., Picas, L., Gazquez, J., Drisko, G.L., Boissiere, C., Grosso, D., Rodriguez-Carvajal, J. & Sanchez, C. (2013). Soft-chemistry-based routes to epitaxial α-quartz thin films with tunable textures. *Science* **340**, 827–831.

Carretero-Genevrier, A., Mestres, N., Puig, T., Hassini, A., Oró, J., Pomar, A., Sandiumenge, F., Obradors, X. & Ferain, E. (2008). Single-crystalline $La_{0.7}Sr_{0.3}MnO_3$ nanowires by polymer-template-directed chemical solution synthesis. *Adv Mater* **20**, 3672–3677.

Carretero-Genevrier, A., Puig, T., Obradors, X. & Mestres, N. (2013). Ferromagnetic 1D oxide nanostructures grown from chemical solutions in confined geometries. *Chem Soc Rev* doi:10.1039/60288e.

Chen, C.T.T., Idzerda, Y.U.U., Lin, H.J.J., Smith, N.V.V., Meigs, G., Chaban, E., Ho, G.H.H., Pellegrin, E. & Sette, F. (1995). Experimental confirmation of the X-ray magnetic circular dichroism sum rules for iron and cobalt. *Phys Rev Lett* **75**, 152–155.

Dagotto, E., Hotta, T. & Moreo, A. (2001). Colossal magnetoresistant materials: The key role of phase separation. *Phys Rep* **344**, 1–153.

Lidbaum, H., Rusz, J., Rubino, S., Liebig, A., Hjörvarsson, B., Oppeneer, P.M., Eriksson, O. & Leifer, K. (2010). Reciprocal and real space maps for EMCD experiments. *Ultramicroscopy* **11**, 1380–1389.

Luo, W., Varela, M., Tao, J., Pennycook, S.J. & Pantelides, S.T. (2009). Electronic and crystal-field effects in the fine structure of electron energy-loss spectra of manganites. *Phys Rev B* **79**, 52405.

Nakagawa, N., Hwang, H.Y. & Muller, D.A. (2006). Why some interfaces cannot be sharp. *Nat Mater* **5**, 204–209.

Rask, J.H., Miner, B.A. & Buseck, P.R. (1987). Determination of manganese oxidation states in solids by electron energy-loss spectroscopy. *Ultramicroscopy* **21**, 321–326.

Rziha, T., Gies, H. & Rius, J. (1996). RUB-7, a new synthetic manganese oxide structure type with a 2×4 tunnel. *Eur J Mineral* **8**, 675–686.

Salafranca, J., Gazquez, J., Pérez, N., Labarta, A., Pantelides, S.T., Pennycook, S.J., Batlle, X. & Varela, M. (2012). Surfactant organic molecules restore magnetism in metal-oxide nanoparticle surfaces. *Nano Lett* **12**, 2499–2503.

Schattschneider, P., Rubino, S., Hébert, C., Rusz, J., Kunes, J., Novák, P., Carlino, E., Fabrizioli, M., Panaccione, G. & Rossi, G. (2006). Detection of magnetic circular dichroism using a transmission electron microscope. *Nature* **441**, 486–488.

Schattschneider, P., Stöger-Pollach, M., Rubino, S., Sperl, M., Hurm, C., Zweck, J. & Rusz, J. (2008). Detection of magnetic circular dichroism on the two-nanometer scale. *Phys Rev B* **78**, 104413.

Varela, M., Findlay, S., Lupini, A., Christen, H., Borisevich, A., Dellby, N., Krivanek, O., Nellist, P., Oxley, M., Allen, L. & Pennycook, S. (2004). Spectroscopic imaging of single atoms within a bulk solid. *Phys Rev Lett* **92**, 095502.

Varela, M., Lupini, A.R., Benthem, K., Van Borisevich, A.Y., Chisholm, M.F.F., Shibata, N., Abe, E., Pennycook, S.J.J., Lupini, A.R. & Borisevich, A.Y. (2005). Materials characterization in the aberration-corrected scanning transmission electron microscope. *Ann Rev Mater Res* **35**, 539–569.

Varela, M., Oxley, M., Luo, W., Tao, J., Watanabe, M., Lupini, A., Pantelides, S. & Pennycook, S. (2009). Atomic-resolution imaging of oxidation states in manganites. *Phys Rev B* **79**, 085117.

Zhang, Z.H., Tao, H.L., He, M. & Li, Q. (2011). Origination of electron magnetic chiral dichroism in cobalt-doped ZnO dilute magnetic semiconductors. *Scr Mater* **65**, 367–370.

Zhang, Z.H., Wang, X., Xu, J.B., Muller, S., Ronning, C. & Li, Q. (2009). Evidence of intrinsic ferromagnetism in individual dilute magnetic semiconducting nanostructures. *Nat Nanotech* **4**, 523–527.